Contribution of the β Subunit M2 Segment to the Ion-Conducting Pathway of the Acetylcholine Receptor†

Hui Zhang and Arthur Karlin*

Center for Molecular Recognition, Columbia University, 630 W. 168th Street, New York, New York 10032

Received January 20, 1998; Revised Manuscript Received March 16, 1998

ABSTRACT: We have applied the substituted-cysteine-accessibility method (SCAM) to the M2 segment and the M1-M2 loop of the acetylcholine (ACh) receptor β subunit. Each residue from βP248 to βD273 was mutated one at a time to Cys, and the mutant β subunits were expressed together with wild-type α, β, and δ subunits in *Xenopus* oocytes. For each of the mutants, the ACh-induced current was near wild-type. The accessibility of the substituted Cys was inferred from the irreversible inhibition or potentiation of ACh-induced current by methanethiosulfonate (MTS) derivatives added extracellularly. Inhibition by MTSethylammonium of βG255C, in the narrow part of the channel, was mainly due to a reduction in the single-channel conductance. Conversely, potentiation by MTSethylammonium of βV266C, in a wider part of the channel, was mainly due to an increase in channel open-time. Two substituted Cys at the intracellular end of M2 and three at the extracellular end were accessible to MTSethylammonium in the absence of ACh. Three additional Cys in the middle of M2 and three in the M1-M2 loop were accessible in the presence of ACh. In the presence of ACh, the secondary structure of βM2 is α-helical from βG255 to βV266 and extended from βL268 to βD273. The accessible residues in βM2 are remarkably hydrophobic, while the accessible residues in the M1-M2 loop are charged. βM2, like αM2, αM1, and βM1, undergoes widespread structural changes concomitant with gating, but the gate itself is close to the intracellular end of the channel. Many aligned residues in the M2 segments of α and β are not identically accessible, indicating that the two subunits contribute differently to the channel lining.

The nicotinic acetylcholine (ACh) receptors are a family of neurotransmitter-gated, cation-selective ion channels. The family contains muscle-type (*1, 2*) and neuronal-type (*3, 4*) receptors. The nicotinic receptor family is a member of a superfamily of homologous neurotransmitter-gated ion channels, including serotonin, γ-aminobutyric acid, and glycine receptors.

The five subunits, $\alpha_2\beta\gamma\delta$, of the muscle-type ACh receptors surround the central channel quasi-symmetrically (*1, 2, 5*). The N-terminal half of each subunit is extracellular, and the C-terminal half forms three membrane-spanning segments (M1, M2, and M3), a large cytoplasmic loop, a fourth membrane-spanning segment (M4), and a short, extracellular tail. The two ACh-binding sites are formed in the extracellular domain in the interfaces between the N-terminal halves of two pairs of subunits, and the channel through the membrane is formed by the membrane-spanning segments of all of the subunits.

Residues lining the ion-conducting pathway have been identified on the basis of the functional effects of mutagenesis and by affinity labeling in the M1 segment (*6*) and the M2 segment (*7*−*11*) of the different subunits. From the effects of mutations of charged residues bracketing M2 on rectification and on the sidedness of channel block by Mg^{2+}, the N-terminal end of M2 was shown to be intracellular and its C-terminal end, extracellular (*9*).

Using the substituted-cysteine-accessibility method (SCAM), in which each residue in and flanking M2 was mutated to Cys and probed with small, charged, sulfhydryl-specific reagents, Akabas et al. (*12*) identified 10 residues in and flanking the M2 segment of the mouse ACh receptor α subunit as channel-lining residues. Also, five residues at the extracellular end of αM1 (*13*) and four residues at the extracellular end of βM1 (*14*) were found to be accessible in the channel. In αM1, βM1, and αM2, the accessibilities of several residues were different in the open and closed states of the channel. It was inferred that the structures of these segments changed during gating and that the gate is at the cytoplasmic end of the channel (*2*).

The sequences of M1 and M2 in the different subunits of the muscle-type ACh receptor are highly conserved (*15*), and the complex is approximately 5-fold symmetrical in the membrane-spanning domain (*5*). Nevertheless, M1 and M2 in the different subunits do not make identical contributions to the channel function (*14, 16*−*18*). Residues in the N-terminal thirds of αM1 and βM1 were found to contribute to the lining of the channel, but these residues in the two subunits did not all align (*14*). The ACh receptor contains only one β subunit. Although β is not directly involved in the formation of the ligand binding sites (*19*), it is required

† Supported in part by research grants from the National Institutes of Health (NS07065), from the Muscular Dystrophy Association, Inc., and from the McKnight Endowment Fund for Neuroscience.

* To whom correspondence should be addressed. Phone: 212-305-3973. Fax: 212-305-5594. E-mail: ak12@columbia.edu.

[1] Abbreviations: ACh, acetylcholine; CFFR, calcium-free-frog-Ringer's solution; dTC, d-tubocurarine; EC_{50}, agonist concentration evoking half-maximal response; MTS, methanethiosulfonate; MTSEA, MTSethylammonium; MTSES, MTSethylsulfonate; MTSET, MTSethyltrimethylammonium; SCAM, substituted-cysteine-accessibility method; WT, wild-type.

S0006-2960(98)00143-3 CCC: $15.00
Published on Web 05/14/1998

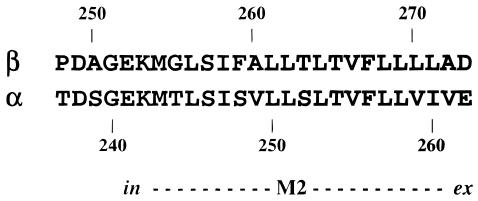

FIGURE 1: The sequence of residues in β mutated to Cys, aligned with residues in α. The residues predicted to be in M2 are indicated by a dashed line. βP248 to βK253 are predicted to be in the M1-M2 loop. *in,* intracellular; *ex,* extracellular.

for the expression of functional receptors at the cell surface (*20*−*23*). We report here on the contribution of βM2 to the ACh receptor channel and on ACh-induced changes in the structure of βM2. We applied SCAM to 26 consecutive residues in βM2 and in the loop between βM1 and βM2 (Figure 1) and identified 11 residues that are accessible in the channel. There are significant differences between the contributions of αM2 and βM2 to the channel lining.

EXPERIMENTAL PROCEDURES

cDNAs for the mouse-muscle ACh receptor subunits were a gift from Dr. Toni Claudio. Residues in and flanking βM2 were substituted by cysteine, one at a time, with the Altered Sites Mutagenesis Kit (Promega). Following mutagenesis, we excised a cassette and ligated it into wild-type in the pSP64T plasmid, cut with the same enzymes. The entire cassette was sequenced to confirm the mutation and ensure that there were no other mutations. Mutants are named as (subunit)(wild-type residue)(residue number)(mutant residue), in which the residues are given in the single-letter code.

The in vitro mRNA transcription, oocytes injection, and two-electrode-voltage-clamp recording of ACh-induced currents were described previously (*12*). The holding potential was −40 mV. The oocytes were perfused at 5 mL/min with nominally calcium-free frog Ringer's solution (CFFR; 115 mM NaCl, 2.5 mM KCl, 1.8 mM $MgCl_2$, 1 μM atropine, 10 mM HEPES, adjusted to pH 7.3 with NaOH), at room temperature.

The methanethiosulfonate (MTS) derivatives, 2-aminoethyl-methanethiosulfonate (MTSEA), 2-trimethylammonioethyl-methanethiosulfonate (MTSET), and 2-sulfonatoethyl-methanthiosulfonate (MTSES) were synthesized as described previously (*24*) and were also purchased from Toronto Research Chemicals (North York, Ontario, Canada). MTSEA, MTSET, and MTSES were applied at concentrations of 2.5, 1, and 10 mM, respectively. The different concentrations compensated for the different rates of reaction of the MTS reagents with simple thiols in solution (*24*).

We tested the susceptibility of wild-type and mutant ACh receptors to the MTS reagents applied in the absence and presence of ACh. The sequence of applications to the oocyte was test concentration of ACh for 10−20 s, CFFR for 3 min, test ACh for 10−20 s, CFFR for 3 min, MTS reagent in CFFR in the absence or the presence of ACh, at a concentration at least 5 times that which gives half-maximal current (EC_{50}), CFFR for 5 min, test ACh for 10−20 s, CFFR for 3 min, and test ACh for 10−20 s. The effects of the reagents on all mutants were tested at two concentrations of ACh, higher than the EC_{50} for the mutant being tested (20 μM or at least three times the EC_{50}, whichever was larger) and at the prereaction EC_{50}. The average of the peaks of the current elicited by two test ACh applications before the MTS reagent was compared with the average peak current elicited by two applications of ACh after the MTS reagent. The effect of the MTS reagent was taken as

$$(I_{\mathrm{ACh,after}}/I_{\mathrm{ACh,before}}) - 1$$

We used the SPSS/PC+ (SPSS, Inc.) statistical software to analyze the effects of MTS reagents by one-way ANOVA, applying the Dunnett test for significance of differences between the effects of MTS reagents on a mutant from the effects on wild-type ($P < 0.05$).

For single-channel experiments, the concentration of mRNA for microinjection varied from 0.02 to 0.2 ng/nL (50 nL/oocyte) in order to obtain a receptor density on the oocyte surface which was optimal for patch-clamp recording. Experiments were performed 2−7 days after injection. The oocytes were checked by two-electrode voltage clamp and were used for single-channel experiments only if they gave maximum ACh-induced currents between 0.5 and 1.5 μA at −40 mV. The oocyte vitelline envelope was removed manually after the oocytes were shrunken in a hyperosmotic solution (150 mM NaCl, 2 mM KCl, 88 mM sucrose, and 5 mM HEPES, pH 7.3). Patch pipets were constructed of thick-walled borosilicate glass (World Precision Instruments, Inc.) with tip-resistance between 12 and 16 MΩ.

By using thick-walled, narrow tips and the outside-out patch configuration (*25*), we found that the incidence of spontaneously active mechanosensitive channels found in *Xenopus* oocyte membrane was very low. If a channel was observed whose open probability increased markedly with depolarization, characteristic of the mechanosensitive channel (*25*−*27*), the patch was discarded. Also, we recorded from every patch for at least 2 min in the absence of ACh and used the patch only if no openings were observed. During these periods, no spontaneous ACh receptor openings were observed.

Single-channel measurements were performed on excised outside-out patches from the animal hemisphere of the oocyte. The pipet solution contained 115 mM KCl, 10 mM HEPES, and 0.5 mM EGTA (pH 7.2), and the bath solution contained 115 mM KCl, 1mM $MgCl_2$, 1 mM $CaCl_2$, and 10 mM HEPES (pH 7.2). All experiments were performed at 20 ± 2 °C. Single-channel currents were measured with a HEKA EPC-9 patch-clamp amplifier and filtered at 10 kHz. The data were stored on videotape through a PCM-2 A/D VCR recorder adapter (44.1 kHz sampling; Medical Systems Corp, Greenvale, NY). Data were played back into a computer, filtered at 2 or 3 kHz with an 8-pole Bessel filter, −3dB, through a DIGIDATA 1200 digital interface (Axon Instruments, Foster City, CA) with a sampling frequency of 20 kHz. Data analysis was performed using pCLAMP software (Axon Instruments, Foster City, CA). Single-channel traces were idealized by using the half-amplitude threshold criterion, and gaps briefer than 100 μs were rejected and adjacent openings concatenated. Open time histograms were plotted using a logarithmic abscissa and a square root ordinate (*28*) and fitted to the sum of one or two exponentials by the method of maximum likelihood. Single-channel conductance was calculated from the slope of the current−voltage curves, usually over the range of −80 to 80 mV. In some experiments, the single-channel conductance was

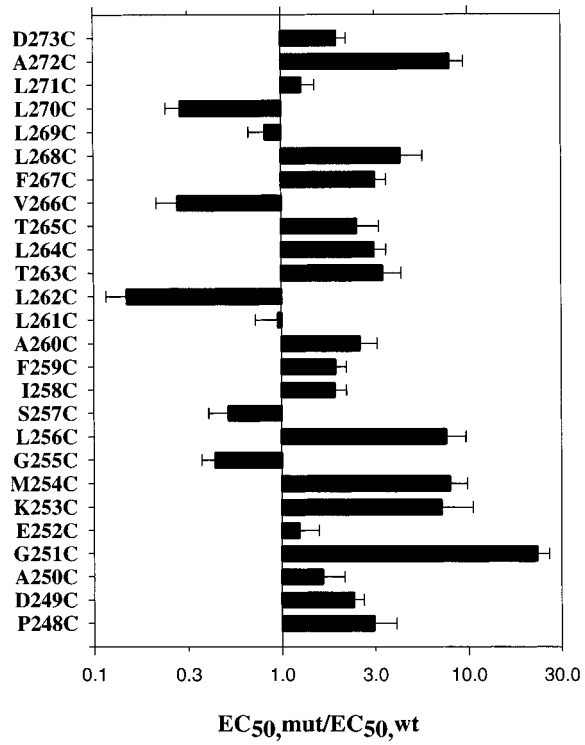

FIGURE 2: The EC_{50} for the Cys-substitution mutants relative to the EC_{50} for wild-type receptor. The EC_{50} was determined from the fit of the Hill equation, $I/I_{max} = 1/[1 + (EC_{50}/[ACh])^n]$, to the currents elicited by five or six different concentrations of ACh, each applied twice. The standard error in the ratio is shown. The number of independent determinations of EC_{50} for each mutant was at least 3. The EC_{50} for wild-type was 1.6 ± 0.2 μM (n = 13). βM254 to βA272 are predicted to be in the M2 segment; βP248 to βK253 are predicted to be in the intracellular loop between M1 and M2.

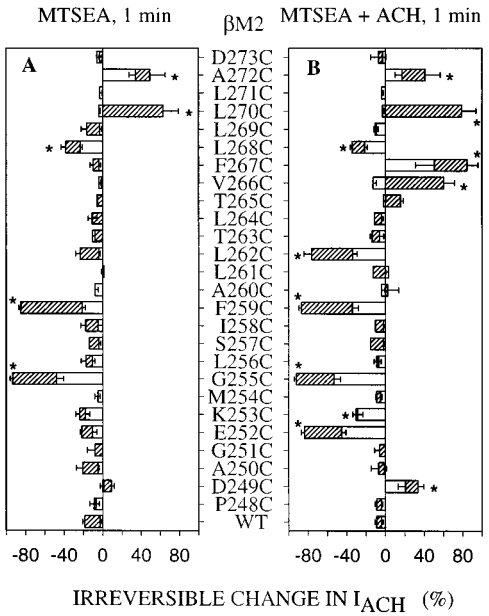

FIGURE 3: Irreversible effects of MTSEA on Cys-substituted β mutants. ACh-induced currents were recorded in oocytes expressing either all wild-type subunits or wild-type α, γ, and δ, and Cys-substituted β subunits. The effects are calculated as $[(I_{ACh,after}/I_{ACh,before}) - 1] \times 100$. The duration of the 2.5 mM MTSEA ($CH_3SO_2SCH_2CH_2NH_3^+$) application and the co-application of ACh (at a concentration ≥5 × EC_{50}) are indicated above the panels. The test concentration of ACh was 20 μM (or 3 × EC_{50}, whichever was greater) (open bars), or the EC_{50} (hatched bars), both plotted from zero. The means and SEMs are shown with SEMs away from zero for hatched bars and toward zero for open bars. For each mutant and condition, at least three oocytes from two independently injected batches were tested. An asterisk indicates that the effect was significantly greater for the mutant than for the wild-type at the level of $P < 0.05$ by ANOVA (Dunnett test).

calculated by dividing the single-channel current by the holding potential. All data are expressed as means ± sem.

RESULTS

Expression of Cys-Substitution Mutants. We inferred that an engineered cysteine reacted if the MTS reagent irreversibly altered the ACh-induced current of oocytes expressing the mutant. We required, therefore, that the cysteine substitution mutants be functional. We found that Cys-substitution was very well tolerated: 25 of the 26 Cys-substitution mutants responded robustly to ACh, with maximum ACh-induced current similar to that of WT (3.0 ± 0.2 μA) with a range from 2.6 ± 0.6 μA for βE252C to 4.2 ± 0.1 μA for βD273C. The ratio, $EC_{50,mut}/EC_{50,wt}$ ranged from 0.15 for βL262C to 7.9 for βM254C (Figure 2). The maximum current of βG251C, 0.43 ± 0.04 μA, was lower than that of the others, and the EC_{50} of this mutant was 23 times larger than $EC_{50,WT}$.

Reaction with MTSEA. In the absence of reagent, the ACh-induced currents were relatively stable over 40 min, the usual duration of an experiment. In wild-type receptor, the change over 40 min in the currents elicited by ACh at its EC_{50} was −4 ± 1% (n = 10). In the mutants, the change over 40 min ranged from +6 to −10%. In wild-type receptor, 2.5 mM MTSEA was applied for 1 min and, in the absence and presence of ACh, caused 19 ± 2% (n = 10) and 10 ± 2% (n = 10) inhibition, respectively. MTSET at 1 mM, applied for 1 min, caused 11 ± 2% (n = 5) irreversible inhibition (Figures 3 and 4). These were the effects tested with ACh at its EC_{50}. The effects on wild-type were smaller when tested at 20 μM ACh. These effects on wild-type served as controls, and the effect on each mutant was tested for statistically significant difference from the effect on wild-type receptor.

The effects of the reagents on each mutant were tested both on the current induced by ACh at 20 μM (or at 3 × EC_{50}, whichever was higher), as in previous work (*12*), and also on the current induced by ACh at its (prereaction) EC_{50}. In all cases, the change in current due to a reaction was larger when tested with ACh at the EC_{50} than with ACh at a concentration higher than the EC_{50}. The basis for the larger effect on the current induced by ACh at the EC_{50} was evident when the reaction shifted the ACh-dose−response curve without changing the maximum response. An example is the reaction of MTSEA with βV266C in the presence of ACh, which caused a 21-fold decrease in the EC_{50} (Figure 5). In this case, current elicited by ACh at the (prereaction) EC_{50} was twice as large after the reaction compared to before the reaction. There was no detectable change in the current induced by ACh at 20 μM, 50 times the prereaction EC_{50}. Testing the effects of reactions on the current induced by ACh at the EC_{50} provided both sensitivity and a consistent basis for the comparison of mutants.

MTSEA was applied extracellularly to 26 Cys-substitution mutants, from βP248C, in the M1-M2 loop, to βD273C, at the extracellular end of M2. The effects on ACh-induced

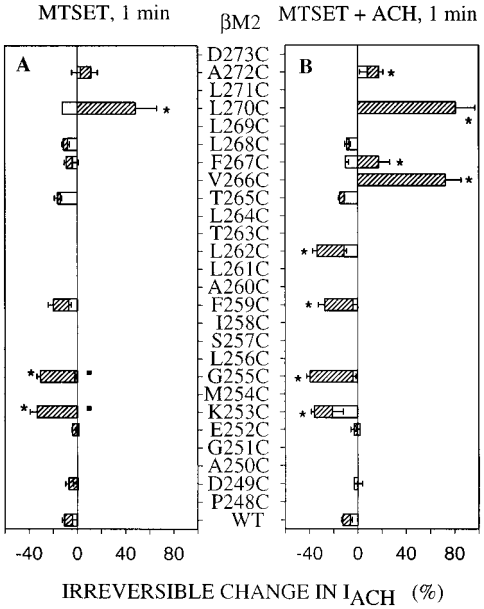

FIGURE 4: Irreversible effects of MTSET on the β mutants susceptible to MTSEA. MTSET (1 mM) [$CH_3SO_2SCH_2CH_2N(CH_3)_3^+$] was applied for 1 min either in the absence or in the presence of ACh. The effects were calculated and represented as in Figure 3. The small black squares next to the bars at G255C and K253C indicate that MTSET was added in the presence of 10 μM d-tubocurarine (dTC) to inhibit its binding to the ACh-binding site.

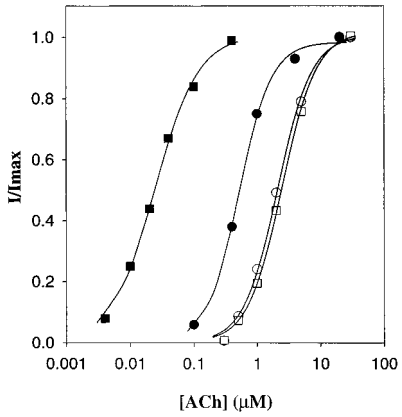

FIGURE 5: The effect of MTSEA on the dose−response curve for ACh. The ACh-induced current at several concentrations of ACh was determined before (circles) and after (squares) application of 2.5 mM MTSEA together with ACh at 10 × EC_{50} for 1 min to wild-type receptor (unfilled symbols) and to βV266C (filled symbols). Plotted are the peak currents (I) during each application of ACh divided by the peak current (I_{max}) elicited by the highest concentration of ACh obtained before the MTSEA application. Lines are fits of the Hill equation to the data.

current were tested with ACh at the EC_{50} (Figure 3, striped bars) and at 20 μM ACh (or 3 × EC_{50}, whichever was greater) (Figure 3, unfilled bars superimposed on the striped bars; all bars start at zero). Both potentiation and inhibition of the current were observed.

In the absence of ACh, in the predominantly closed state of the channel, 2.5 mM MTSEA applied 1 min had statistically significant effects on βG255C, βF259C, βL268C, βL270C, and βA272C, over the entire length of M2 (Figure 3A). The effects on βG255C, βF259C, βL268C, and βA272C were statistically significant when tested at the EC_{50} and at 20 μM ACh (Figure 3A). The effect on βL270C was significant only when tested at the EC_{50}.

In the presence of ACh (≥5 × EC_{50}), when the channels were conducting microamps of current, a 1 min application of 2.5 mM MTSEA had statistically significant effects, tested at the EC_{50}, on βD249C, βE252C, βK253C, βG255C, βF259C, βL262C, βV266C, βF267C, βL268C, βL270C, and βA272C (Figure 3B). The effects on βE252C, βG255C, βF259C, βL262C, and βF267C were also significant when tested at 20 μM ACh. Compared to the effects of a 1 min application of MTSEA in the absence of ACh (Figure 3A), the effects of a 1 min application of MTSEA in the presence of ACh had greater effects on βD249C, βE252C, βK253C, in the M1-M2 loop, and on βL262C, βV266C, and βF267C, from the middle to the extracellular end of M2. (We will call this region the outer half of M2, and the region from the middle to the intracellular end the inner half.) The effects of MTSEA on βD249C and βK253C, in the M1-M2 loop, and on βL262C, βV266C, and βF267C, in the outer half of M2, were significant only when MTSEA was added in the presence of ACh. The effects on βG255C and βF259C, in the inner half of M2, and the effects on βL268C, βL270C, and βA272C, in the outer half of M2, were not much different in the presence and absence of ACh.

Reactions with MTSET. We also examined the ability of MTSET to react with the mutants that were affected by MTSEA. Because of the trimethylammonium group, MTSET is slightly larger and more rigid then MTSEA. MTSET had significant effects only on a subset of the mutants effected by MTSEA.

In the absence of ACh, a 1 min application of 1 mM MTSET had significant effects on βK253C, βG255C, and βL270C (Figure 4A). The effects of MTSET in the absence of ACh are complicated because MTSET acts as a low-affinity agonist of wild-type and of some mutant receptors (*12*). To try to inhibit the binding of MTSET to the ACh-binding site and its activation of the receptor, we added 10 μM d-tubocurarine (dTC) to 1 mM MTSET in the reactions with βK253C and βG255C. Although we do not know (and cannot determine) the EC_{50} for MTSET acting as an agonist on these mutants, 10 μM dTC was insufficient to block all of the current induced by 1 mM MTSET. The effects of 1 mM MTSET with and without 10 μM dTC were approximately the same. (Higher concentrations of dTC were not readily reversed by washing.)

MTSET applied for 1 min in the presence of ACh (at 5 × EC_{50}), significantly affected βK253C, βG255C, βF259C, βL262C, βV266C, βF267C, βL270C, and βL272C (Figure 4B). In the presence of ACh, MTSET reacted with 8 of the 11 mutants that reacted with MTSEA. Only βD249C and βE252C, in the M1-M2 loop, and βL268C, in the outer half of M2, did not appear to react. Despite the weak activation by MTSET alone (or in the presence of dTC), MTSET reacted to a greater extent in the presence of ACh. The ACh-induced increase in reactivity was mainly in the outer half of M2.

A unique consequence of the reaction of MTSET with βV266C in the presence of ACh was that the current persisted after the MTSET and ACh were washed out (Figure 6B). The current approached the baseline with a half-time of about 10 min compared to about 1 min for this mutant before reaction (Figure 6A). Also, the reaction with MTSET caused the EC_{50} to decrease from 0.4 to 0.04 μM ACh (data not shown). The persistence of the activation and the low EC_{50}

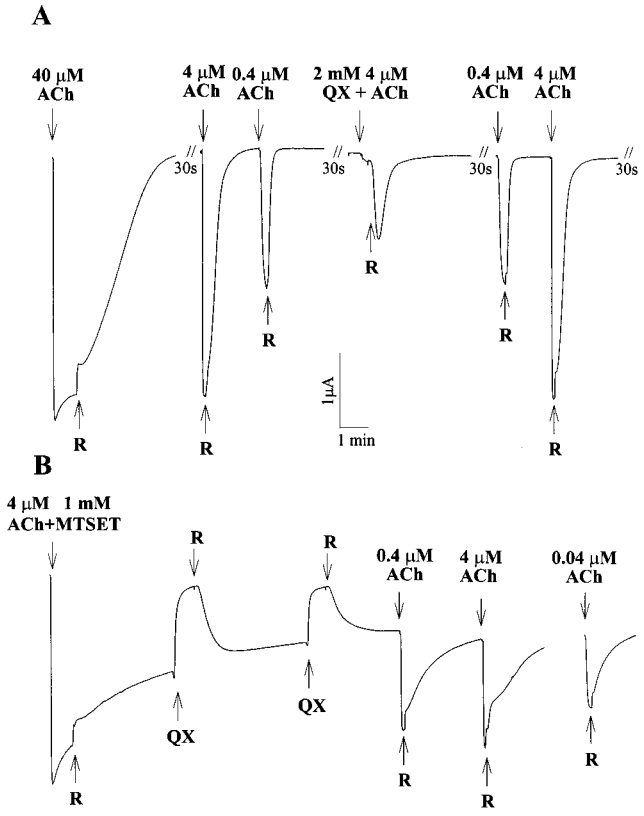

FIGURE 6: Persistence of the open state after the reaction of βV266C with MTSET in the presence of ACh. One continuous experiment is shown with gaps during washes indicated by double slashes. R, CFFR; QX, 2 mM QX-314. The top line (A) shows the current due to various concentrations of ACh and the block of ACh-induced current by QX-314, and the bottom line (B) shows the persistent current following the reaction with MTSET in the presence of ACh and its block by QX-314.

were likely manifestations of the stabilization of the open state of the channel by the addition of the thioethyltrimethylammonium group to the cysteine of βV266C. Consistent with current being due to the persistent activation of the covalently modified receptor, the current was reversibly blocked by 2 mM QX-314 (Figure 6B), which also blocked the current due to 4 μM ACh before MTSET (Figure 6A).[2] The cysteine in βV266C was more exposed to the water-filled channel in the open state than in the closed state, because it was more accessible to both MTSEA (Figure 3) and MTSET (Figure 4) in the presence of ACh, when the channel was highly conductive, than in the absence of ACh, when the channel was closed, and because adding a charged group to the Cys side chain retarded the closing of the channel.

Reactions with MTSES. In the absence of ACh, a 1 min application of the negatively charged MTSES (10 mM) did not affect any of the mutants (Figure 7A). Added in the presence of ACh, 10 mM MTSES reacted with both βL270C

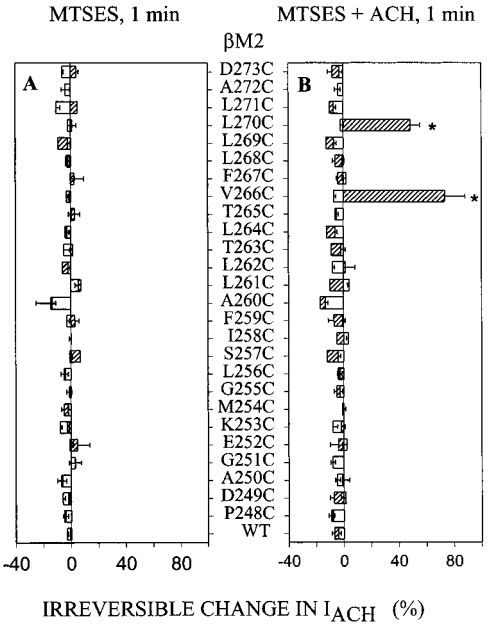

FIGURE 7: Irreversible effects of MTSES on the β mutants. MTSES ($CH_3SO_2SCH_2CH_2SO_3^-$) at 10 mM was applied for 1 min either in the absence or in the presence of ACh at a concentration of $\geq 5 \times EC_{50}$. The effects were calculated and represented as in Figure 3.

and βV266C, potentiating the ACh-induced current (Figure 7B). MTSEA and MTSET had the same effects on these mutants. The lack of an effect of MTSES on other mutants susceptible to MTSEA was in fact due to the lack of reaction and not to a reaction without functional consequences, because after MTSES the application of MTSEA had the same effect as MTSEA added first (data not shown). Thus, the rejection of anions by this cation-selective channel occurs somewhere below βV266. It is not clear, however, why MTSES did not react with βF267C or βA272C, which MTSES must pass in order to get to βV266C.

Reactions of αM2 with the MTS Reagents Tested with ACh at Its EC_{50}. Previously the reaction of substituted-Cys in and flanking the αM2 segment with the MTS reagents was tested at 20 μM ACh (*12*). Three substituted Cys that appeared unreactive when tested at 20 μM ACh were significantly reactive when tested at the EC_{50} for ACh (Figure 8). The reactions of αV259C and αI260C with MTSEA and MTSET, both in the presence and absence of ACh, resulted in significant potentiation of their responses to ACh (Figure 8). In addition, the reaction of αV261C with MTSEA in the presence of ACh and with MTSET both in the presence and absence of ACh resulted in significant inhibition. MTSES, also, reacted in the presence of ACh with αV259C and αI260C. These results imply that five consecutive residues at the extracellular end of αM2, from αL258 to αE262, are exposed in the presence of ACh. It is possible that not all of these are simultaneously exposed in a single α subunit, but rather that different residues are exposed at the extracellular ends of M2 in the two α subunits.

Single-Channel Analysis of Inhibition and of Potentiation by MTSEA. The MTS reagents had inhibitory effects on most of the exposed residues located in the inner halves of αM2 and βM2 and potentiating effects on many of the exposed residues in the outer halves. Given that the modified residues are in the channel and far from the ACh-binding

[2] The ability of 2 mM QX-314 to block the persistent current meditated by βV266C modified by MTSET implies that the covalently attached thioethyltrimethylammonium group does not prevent the binding of QX-314 at high enough concentration. This is consistent with the finding that αV255C, the residue in α that aligns with βV266C, was the outermost residue that was protected by QX-314 against reaction with MTSEA, but this protection was only partial (J. Pascual and A. Karlin, manuscript in preparation). Even in the blocked state, MTSEA could still react with αV255C.

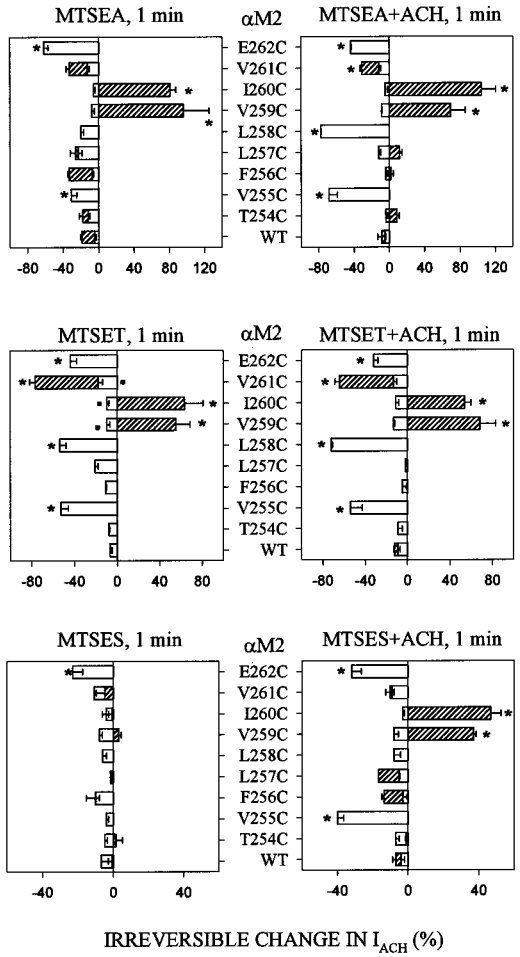

FIGURE 8: Irreversible effects of MTSEA, MTSET, and MTSES on Cys-substitution mutants at the extracellular end of αM2. Reagents were added either in the absence or in the presence of ACh. The effects were calculated and represented as in Figure 3. The small black square next to the bar at αV259C, αI260C, and αV261C indicate that MTSET was added in the presence of 10 μM d-tubocurarine to inhibit its binding to the ACh-binding site. The effects tested with 20 μM ACh are from ref *12*.

sites, the mechanisms for the effects of the modifications likely involve changes in conductance or gating kinetics. We attempted to determine the mechanisms underlying the inhibition of βG255C and the potentiation of βV266C by examining the effects of the reactions on single-channel conductance and kinetics.

The addition of 2.5 mM MTSEA in the presence of 20 μM ACh had no effect on the single-channel conductance, reversal potentials, or the mean open time of wild-type channels (Figure 9 and Table 1). The single-channel conductances and mean open times before and after MTSEA were 52 pS and 2 ms. These values are close to those obtained under similar conditions by others (*29*−*32*).

The mutant βG255C had a slightly smaller single-channel conductance than wild-type, consistent with Cys being larger than Gly and with the location of these residues in the narrow part of the channel (*16*, *17*, *33*, *34*). The reaction of 2.5 mM MTSEA with βG255C resulted in 90% inhibition of the current elicited by 0.7 μM ACh (Figure 3). At the single-channel level, this reaction reduced the conductance of βG255C by 73%, from 46 pS to 12 pS, consistent with the addition of the moiety $-SCH_2CH_2NH_3^+$ to the Cys in this narrow region (Figure 10 and Table 1). The mean open time may have decreased somewhat, although the change was not statistically significant. The effect of MTSEA on the macroscopic current could be largely explained by the decrease in single-channel conductance. The reaction of MTSET with αG255C also reduced the single-channel conductance by about 70% (data not shown).

At the single-channel level, βV266C channels had a mean open time of 13 ms, 6 times the mean open time for wild-type receptor (Figure 11 and Table 1). This difference is consistent with the 3.6-fold decrease in the EC_{50} of the mutant compared to wild-type. The conductance and the reversal potential were the same in wild-type and mutant. The reaction of βV266C with MTSEA in the presence of ACh resulted in a 21-fold decrease in the EC_{50} and, consequently, potentiation in the current elicited by ACh at the prereaction EC_{50}.

The βV266C channel, modified by MTSEA, had unusual properties. First, the modified channel had very long open times (Figure 12A). Some openings lasted for 1−2 s. In the experiment shown, the open-time histogram showed two characteristic open times, a short component of 5 ms (39%) and a new, long component of 294 ms (61%). The average of the longer component in three experiments was 168 ms, 13 times greater than the 13 ms mean open time prior to reaction. Corresponding to the large increase in the mean open time, the open probability after the reaction with MTSEA increased about 10-fold, from 0.015 to 0.15. Even if the mean single-channel current were reduced 2−3-fold because of the subconductance states, with the 10-fold increase in open probability, there would still be an overall increase in macroscopic current of about 3-fold.

Second, the I−V relationship for the full-conductance state showed a slight outward rectification with a slope conductance of 54 pS at positive voltages and 41 pS at negative voltages (Figure 12C). The positive charge introduced on βV266C by the reaction with MTSEA reduced inward conductance but not outward conductance.

Third, in addition to single currents corresponding to the above full conductances, smaller steps of current were frequently observed. Five subconductance states were distinguishable both at positive and negative holding potentials (Figure 12B). The single-channel current stepped between

Table 1: Single-Channel Properties before and after Modification by MTSEA in the Presence of ACh[a]

	before reaction			after reaction		
	γ (pS)	V_{rev} (mV)	τ (ms)	γ (pS)	V_{rev} (mV)	τ (ms)
wild-type	51.8 ± 0.3 (6)	−2.0 ± 0.8 (5)	2.0 ± 0.3 (6)	53.1 ± 1.4 (4)	0.5 ± 0.5 (4)	1.8 ± 0.4 (4)
βG255C	45.9 ± 1.1 (7)	−1.2 ± 1.0 (5)	2.4 ± 0.3 (5)	12.4 ± 0.8 (7)	1.5 ± 0.5 (4)	1.9 ± 0.7 (4)
βV266C	56.7 ± 1.5 (6)	−1.9 ± 1.6 (5)	12.9 ± 2.7 (6)	41.3 ± 0.1 (3)*	−0.5 ± 2.2 (3)	168 ± 74 (3)

[a] The open time (τ) was that of the major component (at least 60% of the events). (*) Conductance at negative voltages; the conductance at positive voltages was 54.0 pS. The numbers in parentheses refer to the numbers of patches.

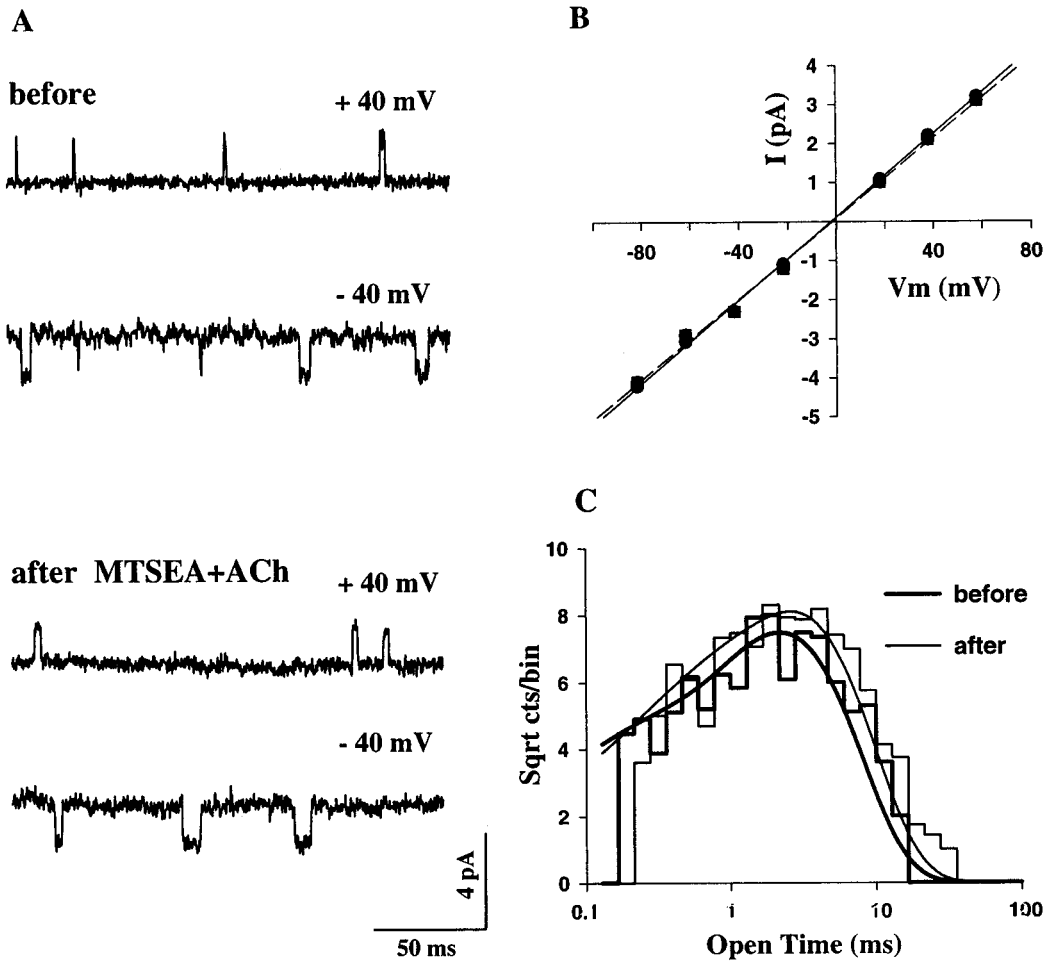

FIGURE 9: Single-channel recording of wild-type receptor before and after the application of MTSEA in the presence of ACh. (A) Recording from an outside-out patch in the presence of 1 μM ACh at holding potentials of 40 mV and −40 mV. Inward currents are shown as downward deflections and outward currents as upward deflections. (B) Single-channel current−voltage relationship before (circles) and after (squares) the application of MTSEA plus ACh. The slope conductance for this recording was 53 pS (before) and 51.4 (after). (C) Open-time histogram fit by the sum of two exponentials with the following parameters: 2.17 ms, 86% and 0.17 ms, 14% (before) and 2.66 ms, 85% and 0.43 ms, 15% (after). Holding potential was −40 mV. Data for panel C were taken from 604 and 735 events, respectively.

these conductance states in equal steps. The steps were likely to reflect substates of a single channel rather than the simultaneous openings of five separate channels with reduced conductances. The sum of the five steps between the subconductance levels was equal to the value of the single conductance in the absence of substates (Figure 12A). Subconductances are rarely observed in wild-type receptor, but these are mostly about 20% of the main conductance (*35*−*39*). In the MTSEA-modified βV266C, the subconductances became dominant. Whether the five steps correspond to the five subunits, and, if so, by what mechanism, are not clear.

We also investigated the mechanism underlining the persistent current after modification of βV266C by MTSET in the presence of ACh. Before the reaction, the probability that the channel would be open in the absence of ACh was $<10^{-4}$. (We estimated this based on the absence of any openings during the 120 s recorded before ACh was added; if there had been on the average one opening, the open probability would have been the mean open time of 12 ms divided by the period of 120 s or 10^{-4}.) After the reaction, the spontaneous open probability increased to 0.03, a value comparable to that of the unreacted mutant in the presence of 0.1 μM ACh. The open-time distribution in the absence of ACh of the MTSET-modified channel was fit by two components, one of 2.1 ms (41%) and another of 23 ms (59%), i.e., both normal and long-lived channels occurred. The reaction also altered the current−voltage relationship, which became inwardly rectifying, with a slope conductance of 58 ± 3 pS at positive potentials and 40 ± 5 pS at negative potentials, as after the reaction with MTSEA.

DISCUSSION

Expression of Cys-Substitution Mutants. Cys is a highly tolerated substitute for other residues (cf., ref *40*). In this and other work (*12*−*14*, and unpublished results), we have tested 105 Cys-substitution mutants in M1, M2, and the M1-M2 loop of both the α and β subunits. Of these 105 mutants, 103 yielded functional receptors at the cell surface. In the present study, each of the 26 Cys-substitution mutants yielded functional cell-surface receptors when expressed in oocytes together with wild-type α, γ, and δ subunits. The functional receptor complex almost certainly contained the mutant β subunits, because very little ACh-induced current is obtained when wild-type mouse-muscle α, γ, and δ are expressed in the absence of β (*22, 23*). Overall, the generally modest effects on the function of the receptor of the Cys-substitutions in βM2 are consistent with similar structures of the mutants and of wild-type receptor.

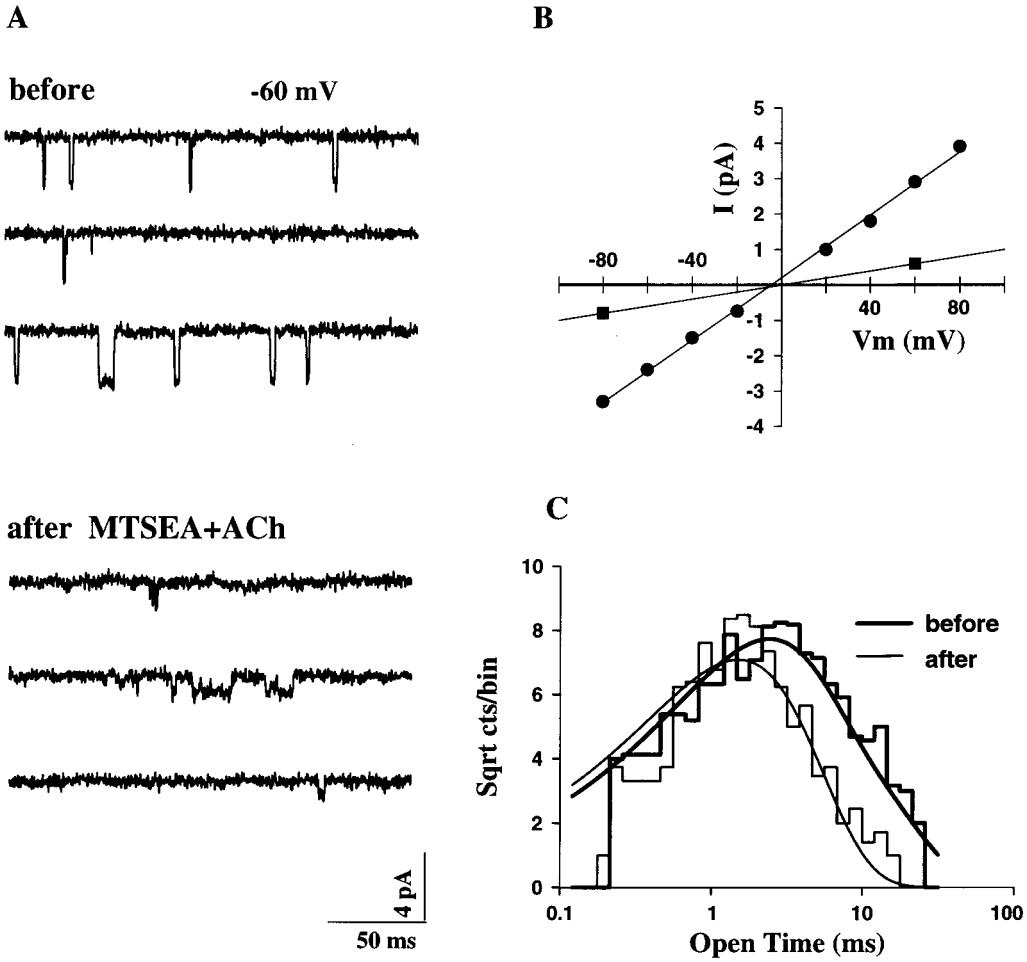

FIGURE 10: Single-channel recording from βG255C before and after the application of MTSEA in the presence of ACh. (A) Recording from an outside-out patch in the presence of 2 μM ACh at −60 mV. (B) Single-channel current−voltage relationship before (circles) and after (squares) the application of MTSEA plus ACh. The slope conductance for this recording was 44 pS (before) and 10 pS (after). (C) Open-time histogram fit by the sum of two exponentials with the following parameters: 2.1 ms, 74% and 5.7 ms, 26% (before); 1.5 ms, 100% (after). Holding potential was −60 mV. Data for panel C were taken from 857 and 646 events, respectively.

Functional States of the Receptor. We have determined whether substituted Cys in the channel react with MTS reagents in the absence and in the presence of ACh. In the absence of ACh, the channel is predominantly closed; the spontaneous open probability is very low (*41, 42*). Immediately upon binding ACh, the receptor undergoes a submillisecond transition from the resting state to the open state. In the continued presence of ACh for tens to hundreds of milliseconds, the receptor enters the fast-desensitized state and then, in tens of seconds, the slow-desensitized state, both nonconducting states (*43*−*47*). The occupied receptor eventually reaches an equilibrium distribution among the different states that favors the slow-desensitized state.

Can we ascribe the reactivities of substituted Cys in the presence and absence of ACh to the open and closed states? MTS reagents were added together with a high concentration of ACh for 1 min. During this time, an unknown fraction of the receptors desensitized. Nevertheless, we customarily recorded microamps of ACh-induced current during the application, and further desensitization was slow (as in the first response to ACh in Figure 6). Thus, the reagents were reacting with some receptors rapidly fluctuating between open and closed states and with some receptors in the desensitized states. Two mutants, αT244C and αK242C, that reacted faster in the immediate presence of ACh than in the absence of ACh, were found to react no faster after prolonged exposure to ACh, when they were desensitized, than they did in the absence of ACh (*48, 49*). For these mutants, at least, the rates of reaction with receptors in the presence of ACh could be taken as a lower limit on the rates of reaction with the open state of the receptor.

Conversely, when the rate of reaction in the absence of ACh is greater or equal to the rate in the presence of ACh, the reaction in the absence of ACh can be associated with the closed state. During the applications of MTSEA and of MTSES in the absence of ACh, no increase in leak current was observed. Even if there were some spontaneous opening of the channels in the absence of ACh (*41, 42*), the fraction of open channels would be far smaller in the absence of ACh than in the presence of ACh, and the contribution of the reaction in the open state to the overall reaction rate would also be very small.

MTSET acts as a low-affinity agonist, and small currents were induced by this reagent in the absence of ACh. Nevertheless, the effects of MTSET on six of eight susceptible mutants were greater in the presence than in the absence of ACh (Figure 4). In these cases, the more current there was, hence more open channels, during the reaction the more reaction.

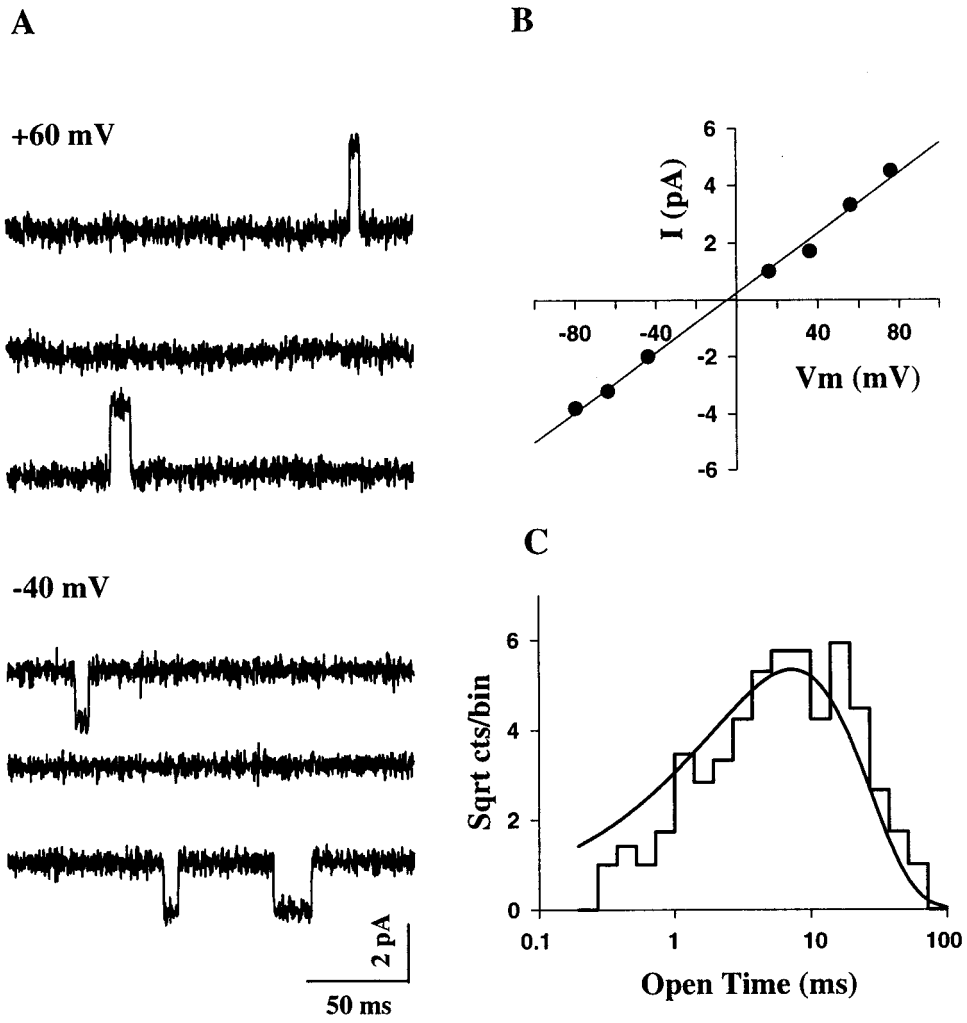

FIGURE 11: Single-channel recording from βV266C. (A) Recording from an outside-out patch in the presence of 0.1 μM ACh at 60 and −40 mV. (B) Single-channel current−voltage relationship. The slope conductance for this recording was 52 pS. (C) Open-time histogram fit by a single-exponential of 7.2 ms. Holding potential was −40 mV. Data for panel C were taken from 234 events.

Channel Lining. The assumptions underlying SCAM and the criteria for judging whether a substituted Cys is accessible have been discussed (*12*, *14*, *50*). On the basis of the effects of a 1 min application of MTSEA in the absence of ACh, five residues in βM2 are exposed in the channel in the closed state (Figure 13, small triangles). In the presence of ACh, eight residues in M2 and three in the M1-M2 loop are exposed in the channel in the open state (Figure 13, large triangles). It is remarkable that seven of the eight side chains contributed by βM2 to the open-channel lining are very hydrophobic (Figure 13, white and yellow, large triangles); only βG255, aligned with three Thr and a Ser in the other subunits, is not especially hydrophobic. The exposed side chains of βM2 do not provide any obvious sites for interaction with ions or with water. The residues in Torpedo ACh receptor aligned with mouse-muscle ACh receptor βG255, βF259, βL262, and βV266 were previously associated with the channel by photolabeling (*1*, *8*, *51*).

In αM2, nine residues are exposed in the channel lumen, of which six are hydrophobic (Figure 13). One of the three exposed polar residues, αT244, is aligned with βG255 and with Thr in γ and Ser in δ, which together contribute to the selectivity of the channel (*16*, *17*, *33*, *34*). The roles of the other two exposed polar residues in αM2 are less clear: αS248 is aligned with αF259, neither of which is crucial for conductance, but each interacts with an open channel blocker (*7*, *52*). The mutation of αS252 to bulkier residues inhibited conductance (*16*); however, the aligned αT263 is not exposed.

Three residues in αM1 (*13*, and unpublished results) and four residues in βM1 (*14*) are exposed in the open channel, and each of these is hydrophobic (although the phenolic −OH of αY213 is a polar group). If we assume that the contributions to the channel lining by γ and δ are similar to those of α and β, the hydrophobicity of the lining above αT244 is remarkable. We do not know, however, the degree of interaction of the backbone peptide groups with ions and water in the channel. These could provide dipolar interactions not evident from the side-chain composition.

In contrast to the M1 and M2 segments, the M1-M2 loop, at the cytoplasmic end of the channel, contains charged residues that are accessible in the open state of the channel (Figure 13). βD249, βE252, and βK253 are accessible from the extracellular medium in the presence of ACh (Figure 3), and αD238, αE241, and αK242 are similarly accessible (*49*). αE241, βE252, and the aligned Gln in γ and Glu in δ constitute the "intermediate ring of charge", which strongly interacts with passing cations (*9*, *53*). αD238, βD249, and the aligned Lys in γ and Asp in δ (the "cytoplasmic ring of charge") also interact with permeating cations, but less

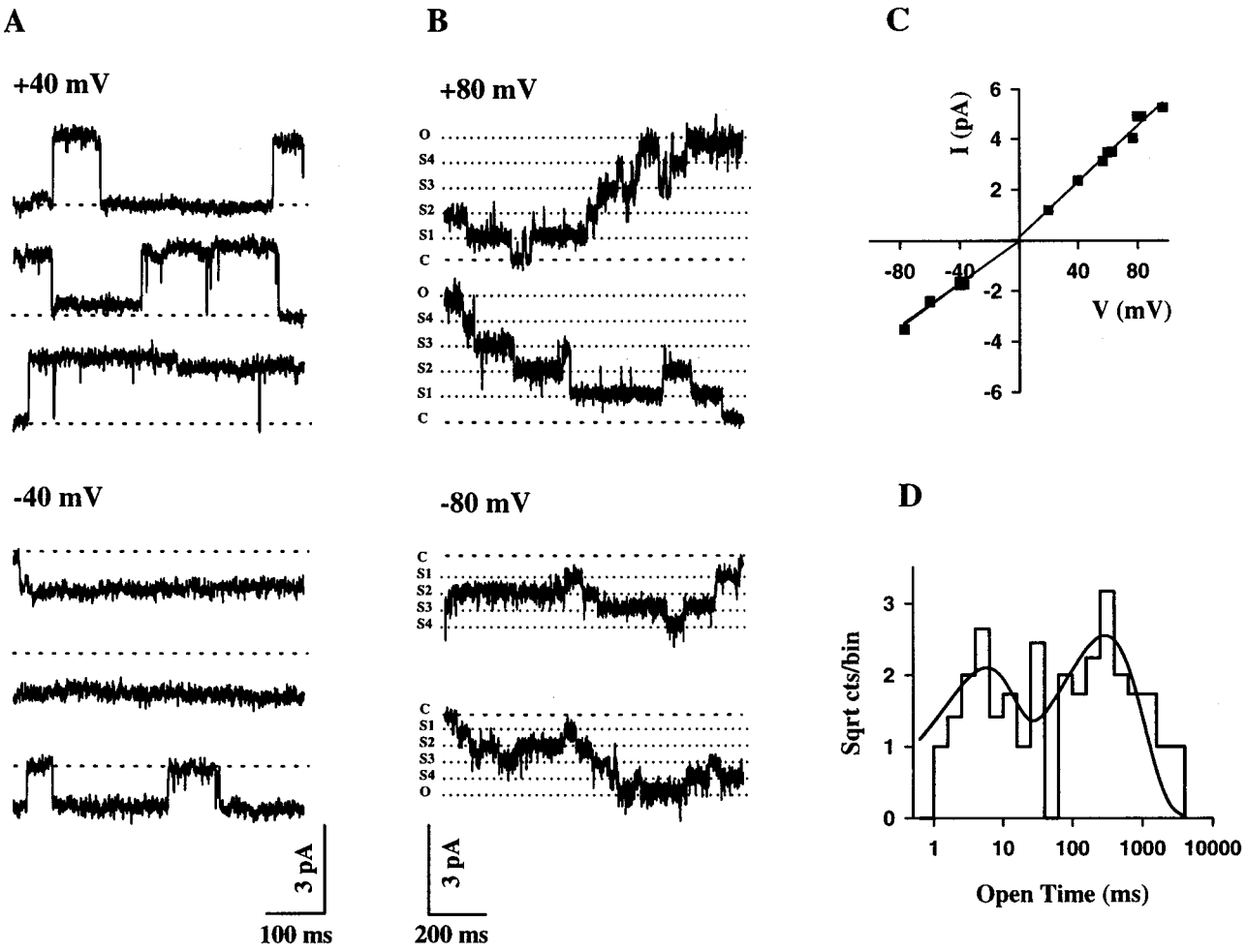

FIGURE 12: Single-channel recording from βV266C after application of MTSEA in the presence of ACh. (A) Recording from an outside-out patch in the presence of 0.1 μM ACh at +40 mV and −40 mV. The dashed line indicates the closed level. (B) Recording showing the multiple substates (dotted lines) in the presence of 0.1 μM ACh at +80 and −80 mV. O, full-conductance level; C, closed state; S, substates. (C) Single-channel current−voltage relationship for the full-conductance state. The currents at negative potentials and the currents at positive potentials were fit separately by straight lines. The mean slope conductances were 54 pS at positive voltages and 41 pS at negative voltages. (D) Open-time histogram fit by the sum of two exponentials with the following parameters: 294 ms, 61% and 5 ms, 39%. Holding potential was −40 mV. Data for panel C are taken from 60 events.

strongly. The role of the five aligned Lys, including αK242 and βK253, is unknown.

The negatively charged MTSES reacted with βV266C in βM2, as with the aligned αV255C, as well as with βL270C, closer to the extracellular end of M2 (Figure 7). MTSES also reacted with βF224C and βY225C in βM1 (*14*) and with αY213C in αM1 (*13*). These results indicate that charge selectivity in this channel begins below the level of αV255C and βV266C. The basis for this charge selectivity might be the negative intrinsic electrostatic potential in the channel (*48*).

Secondary Structure. The pattern of reactivity of substituted Cys in βM2 is compatible with the exposure in the channel lumen of a stripe of regular secondary structure (cf., ref *12*). In the presence of ACh, the accessibility of βG255C, βF259C, βL262C, and βV266C (i.e., every third or fourth residue) in βM2 is compatible with three turns of an α-helix (Figure 13). In the outer third of M2, the accessibility of alternating residues, βL268C, βL270C, and βA272C, is compatible with a β-strand. In αM2, the pattern of reaction in the absence of ACh is compatible with an interrupted α-helix (*12*), while in the presence of ACh the pattern of reaction from αT244 to αL258 is compatible with four turns of an α-helix (Figure 13). Each substituted Cys from αV259C to αE262C reacted with MTSEA. These four residues could form either the exposed last turn of a helix, an extended structure, or different configurations in the two α subunits in the complex.

Structural Changes. In M1 and M2 of α and β, the reactivities of the substituted Cys are different in the predominantly closed state in the absence of ACh and in the open state (and possibly fast desensitized state) in the presence of ACh (Figure 13, triangles at a relative reactivity of 2). Excluding βD249C to βK253C, in the M1-M2 loop, which we consider at or beyond the gate (see below), three of the eight residues in βM2 that reacted in the presence of ACh did not react in the absence of ACh. In βM1, one of four residues that reacted in the presence of ACh did not react in the absence of ACh. There were no residues in these β segments that were more reactive in the absence of ACh than in its presence. By contrast, in the α subunit, there were residues in M1 and M2 that were more reactive in the absence of ACh and others that were more reactive in the presence of ACh. In both α and β, the changes in reactivity induced by ACh occur over the length of the membrane-spanning segments.

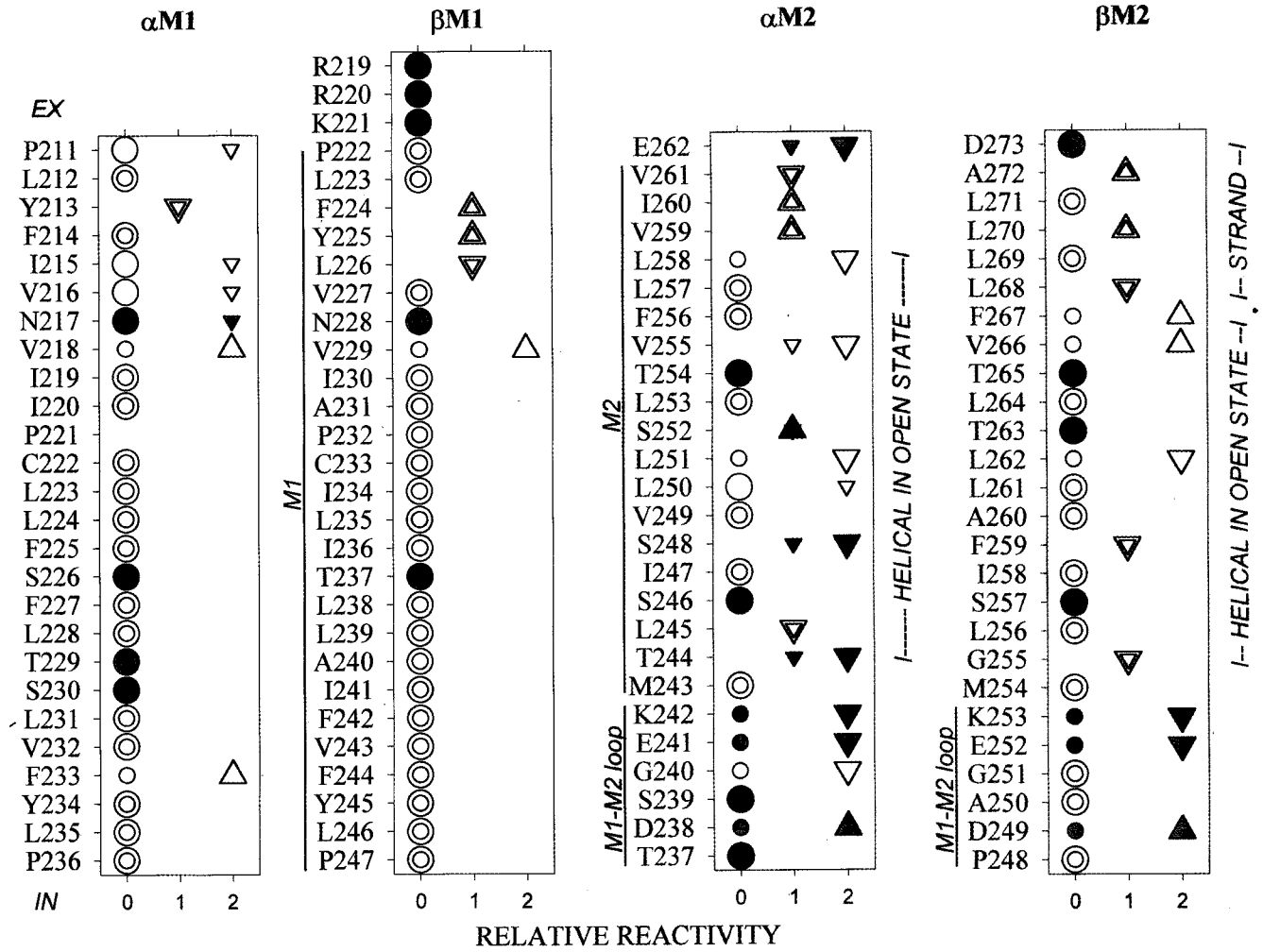

FIGURE 13: Summary of effects of MTSEA on Cys-substitution mutants in and flanking M1 and M2 of the α and β subunits. The sequences of αM1 and βM1 are aligned, and the sequences of αM2 and βM2 are aligned. The M1-M2 loop residues are shown at the bottom of M2. Three residues which flank the extracellular end of βM1 and whose reactivity was tested are shown. Reactivity was determined in the presence and absence of ACh. Small symbols indicate the effects of reaction in the absence of ACh, and large symbols indicate the effects of reaction in the presence of ACh. Circles indicate no detectable reaction; triangles pointing upward indicate potentiation; and triangles pointing downward indicate inhibition. The symbols are plotted at a relative reactivity of 0 if no reaction was detected (all circles), at a relative reactivity of 1 if reaction was detected, and at a relative reactivity of 2 if the reaction in one state was greater than the reaction in the other state. For residues that reacted equally in the presence and absence of ACh, the small symbol is superimposed on the large symbol at a relative reactivity of 1. If the residue did not react in either state the symbols are superimposed at a relative reactivity of 0. If one symbol is at a relative reactivity of 2, the other is at 0 or 1. The symbols at a relative reactivity of 2 indicate the residues, the reactivities of which are different in the presence and absence of ACh. The symbols are color coded for side-chain type: white, aliphatic nonpolar; yellow, aromatic; green, neutral polar; blue, positively charged; red, negatively charged.

In addition to the changes in reactivity of the substituted Cys, the functional effects, first, of the mutation to Cys and, second, of the covalent reaction with the MTS reagents indicate the changing environment of these side chains during ACh-induced conformational changes. The mutations of βL262 to Cys (Figure 2) and of the aligned αL251 to Cys (*12*) resulted in about a 10-fold lower EC_{50}. In both cases, the substituted Cys was much more accessible in the presence of ACh than in its absence. One possibility is that these aligned Leu residues stabilize the closed state by hydrophobic interactions with other residues in the channel wall, which make them less accessible to charged reagents; in the open state, they are more exposed in the water-filled channel lumen. Their mutation to Cys, less hydrophobic than Leu, decreases their stabilization of the closed state and results in a decrease in the EC_{50} (*12, 54*−*57*). Similarly, the mutation of the aligned αV255 and βV266 to Cys also resulted in lower EC_{50}, and these substituted Cys were also more accessible in the presence of ACh than in its absence (Figures 2 and 3; *ref 12*). Furthermore, the reaction of βV266C with MTSEA resulted in a large increase in the mean open-channel time (Table 1), and the reaction with MTSET resulted in a large increase in spontaneous open probability. The mutation to Cys alone decreased the hydrophobicity of the Val side chain, and the addition of the −thioethylammonium moiety to the Cys −SH further increased the polarity of the side chain. Again, these results are consistent with the Val side chains stabilizing the closed state by partly buried hydrophobic interactions and moving into the water-filled channel lumen in the open state. This open-state conformation is stabilized relative to the closed-state conformation when the Val side chains are substituted by more polar side chains.

Examining the effects of the covalent modification of substituted Cys in the channel, we see that potentiating effects (upward pointing triangles in Figure 13) were more likely

to occur in the outer half of the channel, whereas inhibiting effects (downward pointing arrows) were more likely to occur in the inner half of the channel. The potentiating effects were linked to decreases in EC_{50}, which correspond to changes in gating kinetics. In the wider, outer half of the channel (e.g., at βV266C), the detectable reactions with MTS reagents were likely to affect the rates of structural changes involved in gating more than the conductance. In the narrower, inner half of the channel (e.g., at βG255C), the detectable reactions were likely to affect both conductance and gating kinetics.

The Gate. If the gate is a local obstruction in the conduction pathway, then access of the MTS reagents to substituted Cys beyond the closed gate should be blocked. The effects of MTSEA on βF259C and on βG255C are not very different in the presence and absence of ACh. We also know that the spontaneous open probability of βG255C is less than 2×10^{-5} (2 ms/120 s). Thus, the gate is not closer to the extracellular end of the channel than βG255. Similarly, in α, on the basis of the size of the effects (*12*) and of the rate constants (*48*), MTSEA reacts slightly faster with αS248C and slightly slower with αL245C in the presence than in the absence of ACh. Furthermore, the reactions of some charged reagents with αT244C and with αS248C are dependent on the transmembrane electrostatic potential in the presence of ACh but are independent of transmembrane potential in the absence of ACh (*48*). These results also are consistent with a gate closer to the intracellular end of the channel than αT244. Finally, the rates of reaction of α240C, αE241C, αK242C, and αT244C with MTSEA added in the presence and absence of ACh, and extracellularly and intracellularly, indicate that the gate is between αG240 and αT244 (*49*). This is consistent with the greater reactivity in the presence than in the absence of ACh of βK253C, βE252C, and βD249C to extracellular MTSEA (Figure 13).

ACKNOWLEDGMENT

We thank Myles Akabas, Jonathan Javitch, Juan Pascual, and Gary Wilson for their advice and comments on the manuscript and Gilda Salazar-Jimenez for technical assistance.

REFERENCES

1. Galzi, J. L., and Changeux, J. P. (1994) *Curr. Opin. Struct. Biol. 4*, 554−565.
2. Karlin, A., and Akabas, M. H. (1995) *Neuron 15*, 1231−1244.
3. McGehee, D. S., and Role, L. W. (1995) *Annu. Rev. Physiol. 57*, 521−546.
4. Lindstrom, J. (1996) *Ion Channels 4*, 377−450.
5. Unwin, N. (1993) *J. Mol. Biol. 229*, 1101−1124.
6. DiPaola, M., Kao, P. N., and Karlin, A. (1990) *J. Biol. Chem. 265*, 11017−11029.
7. Charnet, P., Labarca, C., Leonard, R. J., Vogelaar, N. J., Czyzyk, L., Gouin, A., Davidson, N., and Lester, H. A. (1990) *Neuron 4*, 87−95.
8. Hucho, F., Oberthur, W., and Lottspeich, F. (1986) *FEBS Lett. 205*, 137−142.
9. Imoto, K., Busch, C., Sakmann, B., Mishina, M., Konno, T., Nakai, J., Bujo, H., Mori, Y., Fukuda, K., and Numa, S. (1988) *Nature 335*, 645−648.
10. Pedersen, S. E., Sharp, S. D., Liu, W. S., and Cohen, J. B. (1992) *J. Biol. Chem. 267*, 10489−10499.
11. Revah, F., Galzi, J. L., Giraudat, J., Haumont, P. Y., Lederer, F., and Changeux, J. P. (1990) *Proc. Natl. Acad. Sci. U.S.A. 87*, 4675−4679.
12. Akabas, M. H., Kaufmann, C., Archdeacon, P., and Karlin, A. (1994) *Neuron 13*, 919−927.
13. Akabas, M. H., and Karlin, A. (1995) *Biochemistry 34*, 12496−12500.
14. Zhang, H., and Karlin, A. (1997) *Biochemistry 36*, 15856−15864.
15. Noda, M., Takahashi, H., Tanabe, T., Toyosato, M., Kikyotani, S., Furutani, Y., Hirose, T., Takashima, H., Inayama, S., Miyata, T., and Numa, S. (1983) *Nature 302*, 528−532.
16. Imoto, K., Konno, T., Nakai, J., Wang, F., Mishina, M., and Numa, S. (1991) *FEBS Lett. 289*, 193−200.
17. Villarroel, A., Herlitze, S., Witzemann, V., Koenen, M., and Sakmann, B. (1992) *Proc. R. Soc. London (B) 249*, 317−324.
18. Cohen, B. N., Labarca, C., Czyzyk, L., Davidson, N., and Lester, H. A. (1992) *J. Gen. Physiol. 99*, 545−572.
19. Blount, P., and Merlie, J. P. (1989) *Neuron 3*, 349−357.
20. Gu, Y., Forsayeth, J. R., Verrall, S., Yu, X. M., and Hall, Z. W. (1991) *J Cell Biol. 114*, 799−807.
21. Kreienkamp, H. J., Maeda, R. K., Sine, S. M., and Taylor, P. (1995) *Neuron 14*, 635−644.
22. Kullberg, R. W., Zheng, Y. C., Todt, W., Owens, J. L., Fraser, S. E., and Mandel, G. (1994) *Recept. Channels 2*, 23−31.
23. Liu, Y., and Brehm, P. (1993) *J. Physiol. (London) 470*, 349−363.
24. Stauffer, D. A., and Karlin, A. (1994) *Biochemistry 33*, 6840−6849.
25. Methfessel, C., V., W., Takahashi, T., Mishina, M., Numa, S., and Sakmann, B. (1986) *Pflugers Arch. 407*, 577−588.
26. Taglietti, V., and Toselli, M. (1988) *J. Physiol. (London) 407*, 311−328.
27. Yang, X. C., and Sachs, F. (1990) *J. Physiol. (London) 431*, 103−122.
28. Sigworth, F. J., and Sine, S. M. (1987) *Biophys. J. 52*, 1047−1054.
29. Liu, E., Hamill, O. P., and Salpeter, M. M. (1994) *Neurosci. Lett. 174*, 77−80.
30. Bouzat, C., and Barrantes, F. J. (1996) *J. Biol. Chem. 271*, 25835−25841.
31. Bufler, J., Kahlert, S., Tzartos, S., Toyka, K. V., Maelicke, A., and Franke, C. (1996) *J. Physiol. (London) 492*, 107−114.
32. Kearney, P. C., Zhang, H. Y., Zhong, W. G., Dougherty, D. A., and Lester, H. A. (1996) *Neuron 17*, 1221−1229.
33. Cohen, B. N., Labarca, C., Davidson, N., and Lester, H. A. (1992) *J. Gen. Physiol. 100*, 373−400.
34. Villarroel, A., Herlitze, S., Koenen, M., and Sakmann, B. (1991) *Proc. R. Soc. London (B) 243*, 69−74.
35. Hamill, O. P., and Sakmann, B. (1981) *Nature (London) 294*, 462−464.
36. Auerbach, A., and Sachs, F. (1983) *Biophys. J. 42*, 1−10.
37. Auerbach, A., and Sachs, F. (1984) *Biophys. J. 45*, 187−198.
38. Colquhoun, D., and Sakmann, B. (1985) *J. Physiol. (London) 369*, 501−557.
39. Morris, C. E., and Montpetit, M. (1985) *Can. J. Physiol. Pharmacol. 64*, 347−355.
40. Kaback, H. R. (1997) *Proc. Natl. Acad. Sci. U.S.A. 94*, 5539−5543.
41. Jackson, M. B. (1989) *Proc. Natl. Acad. Sci. U.S.A. 86*, 2199−2203.
42. Auerbach, A., Sigurdson, W., Chen, J., and Akk, G. (1996) *J. Physiol. (London) 494*, 155−170.
43. Katz, B., and Thesleff, S. (1957) *J. Physiol. (London) 138*, 63−80.
44. Sakmann, B., Patlak, J., and Neher, E. (1980) *Nature 286*, 71−73.
45. Neubig, R. R., Boyd, N. D., and Cohen, J. B. (1982) *Biochemistry 21*, 3460−3467.
46. Heidmann, T., Bernhardt, J., Neumann, E., and Changeux, J. P. (1983) *Biochemistry 22*, 5452−5459.
47. Hess, G. (1993) *Biochemistry 32*, 989−1000.

48. Pascual, J. M., and Karlin, A. (1998) *J. Gen. Physiol.* (In press).
49. Wilson, G. G., and Karlin, A. (1998) *Neuron* (In press).
50. Karlin, A., and Akabas, M. H. (1998) in *Methods in Enzymology* (Conn, P. M., Ed.) pp 123−145, Academic Press, San Diego, CA.
51. White, B. H., and Cohen, J. B. (1992) *J. Biol. Chem. 267*, 15770−15783.
52. Leonard, R. J., Labarca, C. G., Charnet, P., Davidson, N., and Lester, H. A. (1988) *Science 242*, 1578−1581.
53. Konno, T., Busch, C., Von Kitzing, E., Imoto, K., Wang, F., Nakai, J., Mishina, M., Numa, S., and Sakmann, B. (1991) *Proc. R. Soc. London (B) 244*, 69−79.
54. Filatov, G. N., and White, M. M. (1995) *Mol. Pharmacol. 48*, 379−384.
55. Bertrand, D., Galzi, J. L., Devillers-Thiery, A., Bertrand, S., and Changeux, J. P. (1993) *Proc. Natl. Acad. Sci. U.S.A. 90*, 6971−6975.
56. Revah, F., Bertrand, D., Galzi, J. L., Devillers-Thiery, A., Mulle, C., Hussy, N., Bertrand, S., Ballivet, M., and Changeux, J. P. (1991) *Nature 353*, 846−849.
57. Labarca, C., Nowak, M. W., Zhang, H., Tang, L., Deshpande, P., and Lester, H. A. (1995) *Nature 376*, 514−516.

BI980143M